Effects of Zn and Mg in Cu sites of YBa$_2$Cu$_3$O$_{7-\delta}$ single crystals on the resistive transition, fluctuation conductivity, and magnetic irreversibilities

V. N. Vieira

Universidade Estadual do Rio Grande do Sul–UERGS, CEP 95010-005, Caxias do Sul-RS, Brazil

P. Pureur and J. Schaf*

Instituto de Física, Universidade Federal do Rio Grande do Sul–UFRGS, CEP 91501-970, Porto Alegre-RS, Brazil

We report on the resistive transition and fluctuation conductivity of an YBa$_2$Cu$_{2.97}$Zn$_{0.03}$O$_{7-\delta}$ single crystal and on the magnetic irreversibilities of this compound in two different oxygen states and another YBa$_2$Cu$_3$O$_{7-\delta}$ single crystal in which (1 at. %) of Cu was substituted by Mg. Our measurements show a very drastic decrease of the superconducting transition temperature and the growth of granularity effects already in this low dopand concentration. In the temperature region immediately above T_c our results of fluctuation conductivity reveal the occurrence of critical and Gaussian regimes. The resistive transition of the YBa$_2$Cu$_{2.97}$Zn$_{0.03}$O$_{7-\delta}$ single crystal occurs in two steps. First superconductivity sets in within the grains and at somewhat lower temperature long-range superconducting order takes place over the whole sample. Between the zero resistance temperature $T_{c0}(H)$ and the pairing transition temperature $T_c(H)$ lays the magnetic irreversibility line $T_{irr}(H)$, which follows the power law predicted by the flux creep theories in most of the high field range. However, in a low field region, dominated by Josephson flux dynamics, the irreversibility line exhibits two different regimes dominated by disorder and frustration and characterized by AT (de Almeida-Thouless) and GT (Gabay-Toulouse) power law behaviors. This Josephson flux dynamics is squeezed into a considerably smaller field region than in other granular YBa$_2$Cu$_3$O$_{7-\delta}$ systems. We attribute the origin of the observed stepwise resistive transition and low field magnetic irreversibility regimes mainly to the granularity of the superconducting state, which is induced by the impurities at the Cu sites and increased by shortage of oxygen.

I. INTRODUCTION

The relation existing between the chemical structure of the high-temperature superconductors (HTSC's) and the topology of the Ginzburg-Landau (GL) order parameter have provided important insights about the nature of the superconducting state of these materials. For instance, studies of the effects of impurities on known sites have been extensively used during the last decade as a tool to study the origin of superconductivity in these materials.

The techniques of the differential anomalous x-ray scattering,[1] the x-ray absorption near edge,[2] and the x-ray diffraction,[3-10] have been used to locate the impurities in the crystal lattice. Zinc impurities in the YBa$_2$Cu$_3$O$_{7-\delta}$ (YBCO) host were found to substitute preferentially the Cu atoms of the CuO$_2$ planes up to concentrations near 1 %,[1,2,4,5] while Mg ions substitute Cu in the CuO$_2$ planes as well as in the Cu-O chains up to about the same concentration.[6-9] The reason why the Zn and Mg impurities prefer the Cu sites lies in their reduced ionic radius (0.75 and 0.65 Å respectively) that closely match that of the Cu ions (0.72 Å).

On the other hand, more specific studies of the superconducting properties of Zn and Mg doped YBCO samples, by resistivity and magnetoresistance,[3,4,7,8] magnetization and NMR,[10,11] ac-magnetic susceptibility, and magneto-resistance[9] gave account of drastic effects of Cu substitutions on the superconducting properties of this compound. This contrasts with the relatively moderate effects of Sr or Ca substitution at the Ba sites or the even much more subtle effects of rare earth impurities at the Y site. Moreover, the effects of Zn impurities on the electronic charge density redistribution,[12] muon spin relaxation rate,[13,14] superconducting coherence length,[15] normal state Hall angle,[16] specific heat,[17,18] as well as on the correlation between magnetic and superconducting properties[19] play an important role in unveiling the superconducting morphology of these materials. The dramatic depression of T_c (Refs. 20 and 21) and the large anisotropy of the normal resistivity, coherence length[22] and penetration length[23,24] of YBCO single crystals doped with Zn or Mg were soon considered as strong evidences that the CuO$_2$ planes of the orthorhombic perovskite structure are the main responsible for the superconductivity in these materials. This planar structure is now known to be a quite general characteristic of the HTSC and to govern a number of its intrinsic properties. However, the exact reason why Zn and Mg impurities depress so drastically the critical temperature of YBCO is still unclear. Several doubts concerning the specific effect of substitutional Zn and Mg at the Cu sites on the coherence length[15,22] and pair breaking effects[3,15] remain to be cleared up. Zinc impurities, although not causing an observable overall charge carrier redistribution,[2,12] cause strong electron scattering originating local inhomogeneity in carrier concentration. The induction of small magnetic moments on neighboring Cu atoms is often considered as a contribution to the T_c depression,[6,10] but the main cause probably is an effect of nonmagnetic quasiparticle scattering

in d wave superconductors with the appearance of new states within the superconducting gap.[9]

Contrasting with the rich literature on several normal and superconducting properties of YBCO doped with Zn or Mg, only one detailed study of the resistive transition of a Zn doped polycrystalline sample is available.[25] Practically nothing is known about the effects of superconducting fluctuations on the electrical conductivity near T_c and the overall behavior of the magnetic irreversibility. Both of these properties can give important insights into the mesoscopic morphology of the superconducting state of these materials. In the present work we report on the results of very detailed studies of the low field resistive transition, the fluctuation conductivity and the magnetic irreversibility for fields applied along the c axis as well as along the ab plane. The magnetoresistivity measurements of a well oxygenated $YBa_2Cu_{2.97}Zn_{0.03}O_{7-\delta}$ single crystal show a granular superconducting character and several different regimes of fluctuation conductivity. The magnetic irreversibility lines of this same sample as well a of an $YBa_2Cu_{2.97}Zn_{0.03}O_{7-\delta}$ single crystal of the same batch having a lower oxygen content and of a $YBa_2Cu_{2.97}Mg_{0.03}O_{7-\delta}$ single crystal. The magnetic irreversibilities of all samples corroborate the predictions of the conventional flux creep model in fields above 2 kOe. However, in a low field region they clearly display the characteristics of the Josephson flux dynamics in a frustrated granular superconductor.[26]

II. SAMPLE PREPARATION AND EXPERIMENTAL PROCEDURES

The doped $YBa_2Cu_{2.97}M_{0.03}O_{7-\delta}$ ($M=Zn$ or Mg) single crystals were grown by the CuO flux method. The highly pure Y_2O_3, $BaCO_3$, CuO, and ZnO or MgO powders were heavily ground in a agate mortar in the proportions 1:4:9.9:0.1 of Y, Ba, Cu, and M, respectively. Subsequently the mixture was piled up on the higher side of a ZrO_2 tray tilted 15° and slowly heated in air from room temperature to 1020 °C during 10 h. The temperature was held at 1020 °C for 1 h and then slowly lowered to 900 °C in 48 h. Subsequently the furnace was cooled slowly past 700 °C and then down to room temperature. During this temperature processing the saturated flux flows out from the mixture down to the lower side of the tray. The doped YBaCuO single crystals grow out from the slowly evaporating flux in the lower side of the tray incorporating the Zn or Mg impurities at Cu sites. The solubility of Zn (Ref. 2 and 20) and/or Mg (Ref. 6 and 9) is rather good within the range of low concentrations (1 at. %) of our samples. The crystals can be easily removed as they normally stick free upon the surface of the flux attached to it only along the border. In a second round, the single crystals were encapsulated between two polycrystalline YBCO-123 mini-dishes and oxygenated in pure flowing oxygen at 450 °C. One $YBa_2Cu_{2.97}Zn_{0.03}O_{7-\delta}$ single crystal [YBCO(Zn)S1], treated during seven days, was underdoped with oxygen. Another single crystal of the same batch [YBCO(Zn)S2] and a Mg doped single crystal were treated during ten days and achieved a maximum of oxygen content. In
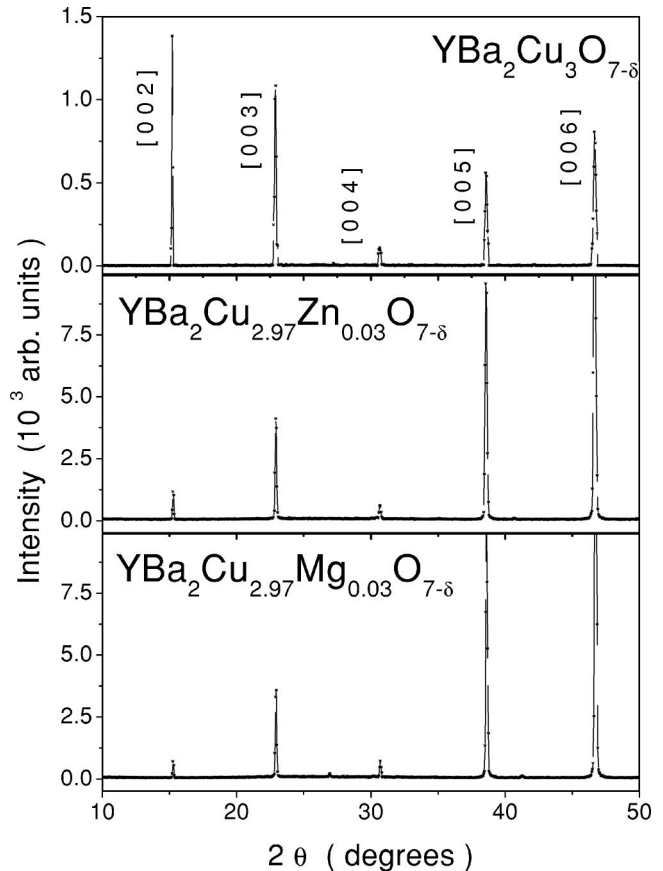

FIG. 1. X-ray diffraction spectra of a pure $YBa_2Cu_3O_{7-\delta}$ single crystal and our Zn and Mg doped single crystals, obtained for monochromated Cu$K\alpha$ radiation incident along the c axis of the crystals. No relevant strange phases are visible in the samples.

a final step the samples were slowly cooled to room temperature.

Our main experimental techniques were magnetoresistivity and dc magnetization. However, other techniques were also used to analyze the samples. X-ray diffraction showed only the pure orthorhombic phase (see x-ray spectra in Fig. 1) and lattice parameters in agreement with those in the literature for 1 at. % of the Cu atoms replaced by Zn or Mg.[2,6] The superconducting transition temperatures T_c were determined from the first inflection of low field dc magnetization curves as shown in Fig. 2, and are in agreement with those reported in the literature.[9] To perform the magnetoresistivity and dc magnetization measurements we selected single crystals of very clean appearance having a nearly rectangular shape of about 1 mm² in area, and 0.1 mm in thickness. The ab plane of the crystals could be aligned along the field orientation to within 1° of precision.

The magnetoresistivity measurements were made with a four contact technique employing a low current-low frequency ac experimental setup in which a lock in amplifier is used as a null detector. The temperature was measured with a Pt resistor, corrected for magnetoresistance effects, within a resolution of 2×10^{-3} K. During the measurements, the temperature was swept very slowly (0.05 K/min) so that a high number of data points could be recorded in the temperature
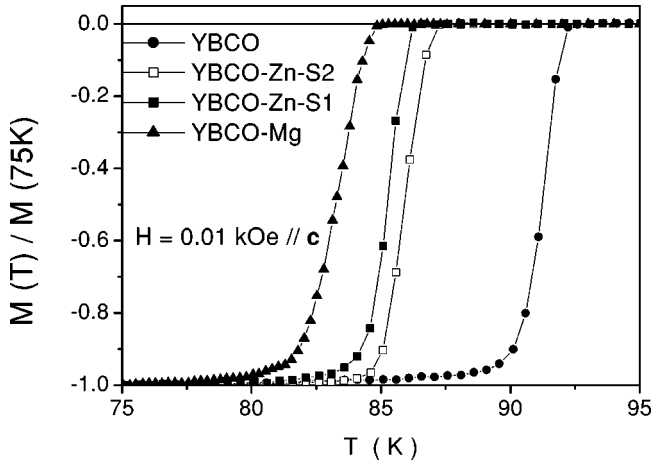
FIG. 2. Low field zero-field-cooled dc magnetization curves of the pure YBCO-123 single crystal (Ref. 55), of the $YBa_2Cu_{2.97}Zn_{0.03}O_{7-\delta}$ single crystals treated under pure oxygen at 450°C during 7 days [YBCO(Zn)S1] and during 10 days [YBCO(Zn)S2] and the $YBa_2Cu_{2.97}Mg_{0.03}O_{7-\delta}$ single crystal [YBCO(Mg)]. The onset of diamagnetism is approximately the pairing temperature, T_c.

range near the transition and the temperature derivative of the resistivity ($d\rho/dT$) could be numerically determined.

The magnetic irreversibilities were obtained from dc magnetization measurements using a SQUID (superconducting quantum interference device) MPMS-XL magnetometer from Quantum Design. The method consisted in first cooling down the sample to temperatures well below T_c in zero magnetic field (ZFC), then measuring the magnetization (M_{ZFC}) while slowly warming (0.2 K/min or less) up to $T \gg T_c$ in a stable field, and subsequently measuring M_{FC} while slowly cooling back (FC) in the same field. In order to improve the evaluation of the magnetic irreversibility limit, we subtracted M_{ZFC} from M_{FC} for a given field value, generating the array $\Delta M = M_{FC} - M_{ZFC}$. The irreversibility limit (T_{irr}), for a given applied field, is given by the temperature point where the ΔM data abandon the zero base line, defined by the data in the reversible upper temperature region. While in high fields ($H > 10$ kOe) T_{irr} could be determined to within 0.5 K or better, in the lowest fields this precision improves to 0.2 K or better. On the other hand, the applied field could be read to within a fraction of an Oersted after correcting for the remanent field of the superconducting coil. Although the $M_{FC}-M_{ZFC}$ magnetization method is the most precise one, it can be significantly affected by temperature gradients because of its intrinsic temperature cycling. In the case of superconductors, these temperature gradients are modulated by the variable thermal conductivity of the materials near T_c. On the other hand, the automatic sample centering facility, so useful in magnetometers with pick up coils, may fail when the longitudinal moment of the sample becomes too small near the crossover from diamagnetism to paramagnetism, resulting in data distortions in the zero-moment crossing region. All these effects are very misleading if not adequately by-passed. We have first minimized the temperature gradients (to less than 0.1 K) by using appropriated experimental procedures, then carefully studied the residual terms in order
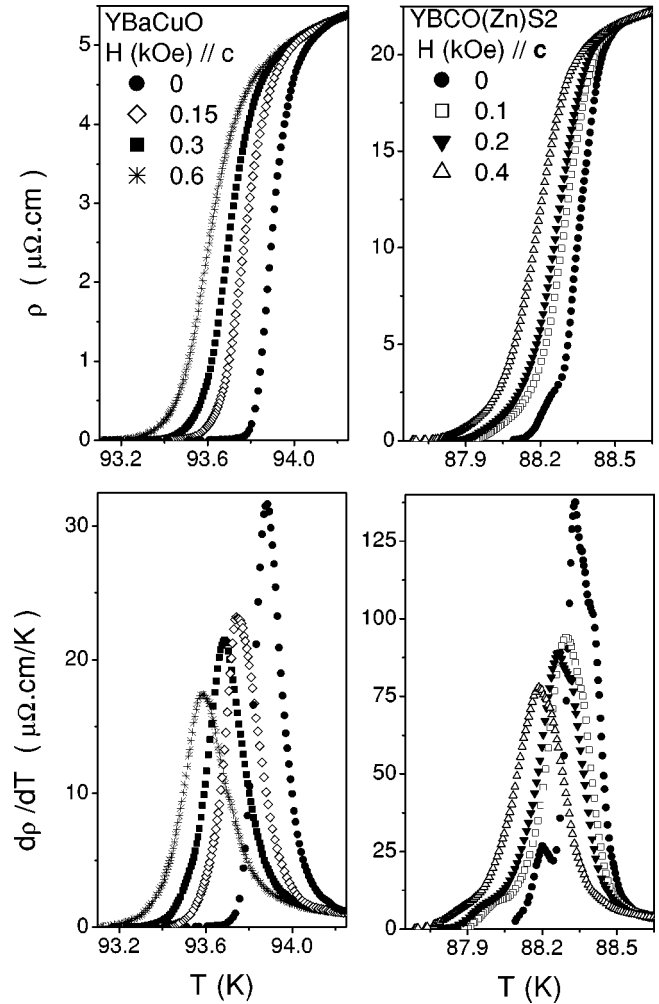

FIG. 3. The characteristic resistive transitions (upper panels) and temperature derivatives (lower panels) of the pure YBCO-123 single crystal (left) and of the YBCO(Zn)S2 single crystal (right). Remark that even low fields smooth down the characteristic feature of the coherence transition.

to develop an analytical method for further corrections. We also used a zero suppress technique to prevent the magnetic signal from crossing zero.

III. EXPERIMENTAL RESULTS AND DISCUSSION

A. Resistive transition

In order to examine the topology of the superconducting state (granularity) and the nature of the superconducting transition in the studied systems, we made detailed magnetoresistivity measurements on one of our samples. These measurements also yielded useful information on the fluctuation conductivity above T_c as well as on the occurrence of a coherence transition below T_c. These measurements were performed as a function of temperature within the configurations $H\|ab$ or $H\|c$ and measuring current along the ab plane ($J\|ab$) for several values of the applied field in the range 0 to 1 kOe. The upper left-hand panel of Fig. 3 displays the resistive transition at several fields oriented along

the c axis for the nearly perfect YBCO-123 single crystal from Ref. 26, while the upper right-hand panel shows similar results for the YBCO(Zn)S2 single crystal. There it can be observed that the resistive transition of the YBCO-123 single crystal is a single step process, while that of the doped sample occurs in two steps. In order to make a closer examination of these resistive transitions, we show in the lower panels of Fig. 3 the respective temperature derivatives $d\rho/dT$. The transition of the pure single crystal appears as a single sharp peak in $d\rho/dT$. Instead the YBCO(Zn)S2 sample displays, besides a main peak, a satellite or hump at the lower-temperature side. The main peak is barely affected by an applied field and marks the position of the pairing critical temperature T_c. The secondary hump is strongly affected by the field and is the usual signature of granular superconductors.[26,27] These features show that the pure single crystal behaves as a single grain and has no junctions at all. The doped crystal is, however, formed by several superconducting grains that are connected by weak links of nearly the same strength. We suggest that granularity in this case results from a random distribution of oxygen rich superconducting regions that are embedded in a weaker superconducting or nonsuperconducting background material.

B. Fluctuation conductivity

The superconducting fluctuations induce detectable contributions to the electric conductivity, σ of the HTSC. In a significant temperature range above T_c, the normal conductivity, σ_N of our samples is dominated by fluctuations and behaves as [see inset in panel (a) of Fig. 3]

$$\sigma_N(T) = (aT + b)^{-1}, \tag{1}$$

where a and b are sample dependent phenomenological constants. Assuming that Eq. (1) describes the regular contribution to the conductivity of our samples, we extrapolate this behavior to the transition region in order to estimate the excess electric conductivity, $\Delta\sigma$ caused by thermal fluctuations

$$\Delta\sigma = \sigma - \sigma_N, \tag{2}$$

where $\sigma = \rho^{-1}$ and $\sigma_N = \rho_N^{-1}$ Assuming that $\Delta\sigma$ diverges according to a simple power law

$$\Delta\sigma = A(T - T_c)^{-\lambda}, \tag{3}$$

where A is a critical amplitude and λ is a critical exponent when the temperature approaches T_c from above, we calculate the temperature derivative of $\ln(\Delta\sigma)$,

$$\chi_\sigma(T) = -\frac{d}{dT}\ln(\Delta\sigma) \tag{4}$$

and plot

$$\chi_\sigma^{-1}(T) = -\frac{1}{\lambda}(T - T_c). \tag{5}$$

The existence of asymptotically critical fluctuation regimes becomes evident in the $\chi_\sigma^{-1}(T)$ plots if a linear behavior of the data over considerable temperature intervals can be
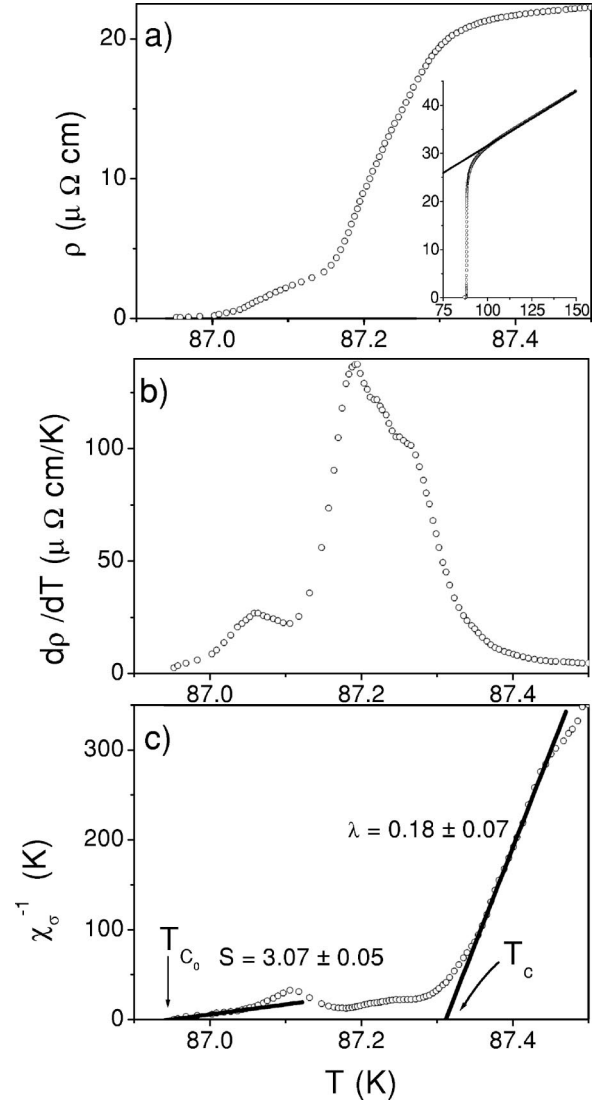

FIG. 4. The resistive transition, the temperature derivative and the $\chi_\sigma^{-1}(T)$ plot of the YBCO(Zn)S2 single crystal under zero applied field. The straight line through the $\chi_\sigma^{-1}(T)$ data labeled $\lambda = 0.18 \pm 0.07$ is a fitting to Eq. (5) and the one labeled $S = 3.07 \pm 0.05$ is a fitting to Eq. (6).

found. In general several fluctuation regimes, characterized by well defined values of the exponent λ can be identified.[28]

The panels (a), (b), and (c) in Fig. 4 display the resistive transition of our Zn doped single crystal, represented respectively as ρ, $d\rho/dT$, and $\chi_\sigma^{-1}(T)$ curves in a narrow temperature range encompassing T_c in zero applied field. The two steps character of the resistive transition in this sample is rendered evident in these representations. The straight line through the $\chi_\sigma^{-1}(T)$ data at the right hand side in panel (c), labeled by the exponent $\lambda \sim 0.18 \pm 0.07$, is a fitting to Eq. (5). This is the asymptotic critical fluctuation regime found in this sample. Extrapolation of this fitting to the temperature axis yields the best evaluation of the pairing critical temperature ($T_c = 87.31$ K).

An applied magnetic field affects considerably the superconducting transition and the fluctuation regimes in the immediate vicinity above T_c. In Fig. 5 we show $\chi_\sigma^{-1}(T)$ data
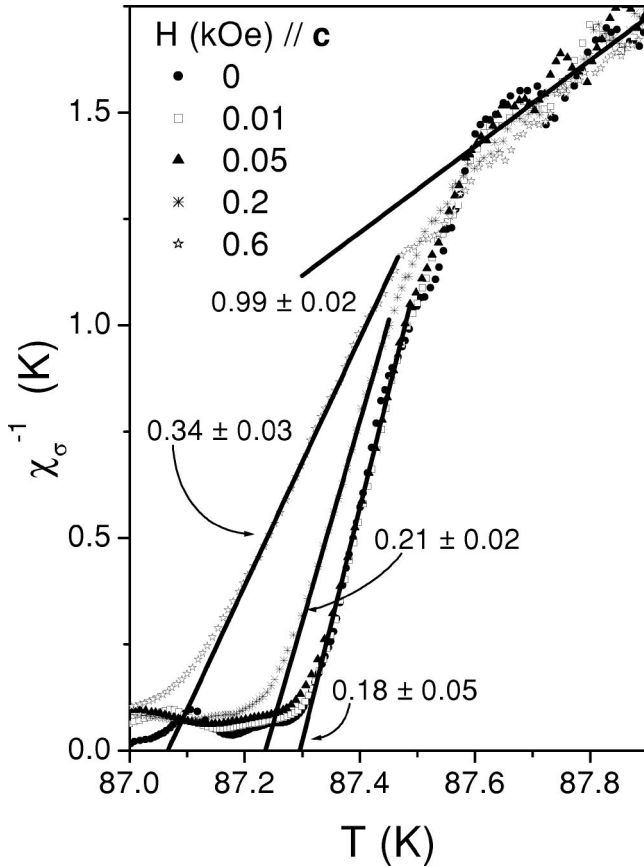
FIG. 5. Plots of the $\chi_\sigma^{-1}(T)$ data for $H\|c$ for the YBCO(Zn)S2 single crystal under several applied fields, showing the evolution of the asymptotic critical regime in the immediate vicinity above T_c with increasing applied field until the 3D-XY regime. The straight lines through the data, labeled $\bar{\lambda}=0.18, \lambda=0.21$ and $\lambda_{cr}=0.34$ are fittings to Eq. (5).

closely above T_c under several fields between 0 and 0.6 kOe applied along the c axis. As shown by the straight lines through the data, at the lowest fields and up to 0.05 kOe, the asymptotic critical regime corresponds to the exponent $\bar{\lambda}=0.18\pm0.05$ (averaged over the three lowest fields). When the field is further increased, the value of this exponent crosses over to $\lambda=0.21\pm0.02$. Finally, in $H=0.6$ kOe, the exponent corresponding to the asymptotic critical regime reaches the expected three-dimensional XY (3D-XY) value, ($\lambda_{cr}=0.34\pm0.03$). In fact, when the $\chi_\sigma^{-1}(T)$ data are carefully analyzed, the 3D-XY regime may be discerned immediately above the asymptotic scaling in lower applied fields. The behavior depicted in Fig. 5 is reproduced when the magnetic field is applied parallel to the ab plane but for somewhat higher fields. Farther from T_c the $\chi_\sigma^{-1}(T)$ data may be fitted to Eq. (5) with a field independent exponent $\lambda_G^{(2D)}=1.0$, which is expected when $\Delta\sigma$ is dominated by two-dimensional Gaussian (2D-G) fluctuations. Increasing further the temperature above T_c, another extended power law regime in $\Delta\sigma$ may be discerned in $\chi_\sigma^{-1}(T)$ plots, as exemplified in the representative results of Fig. 6. The value for the corresponding exponent, $\lambda_G^{(1D)}=1.5$, suggests the occurrence of one-dimensional Gaussian (1D-G) fluctuations. The expo-
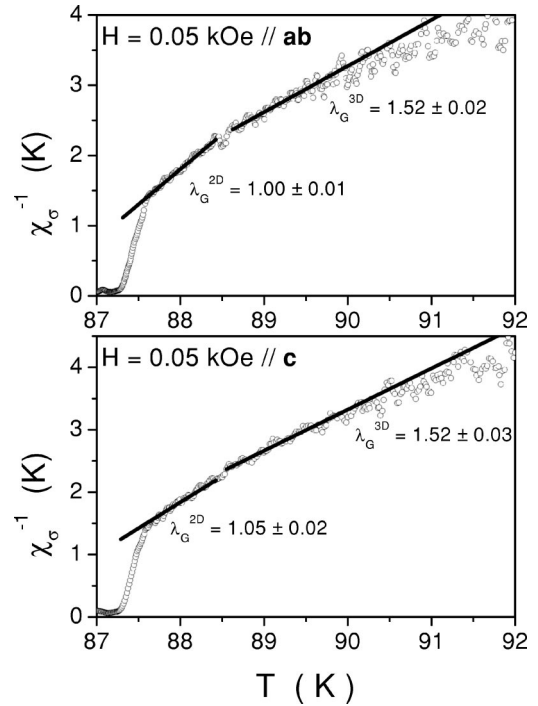

FIG. 6. The same as in Fig. 5, but for a temperature region farther away from T_c and for the indicated applied field. 2D and 1D Gausssian fluctuation regimes, characterized by the critical exponents $\lambda_G^{(2D)}=1$ and $\lambda_G^{(3D)}=1.5$, are identified for $H\|c$ and $H\|ab$. The straight lines are fittings with Eq. (5).

nents and amplitudes characterizing the 2D-G and 1D-G regimes are robust against the field magnitude, for both field orientations, up to the highest field value, investigated in this work (0.6 kOe) and beyond, to be published.

As the temperature is decreased below T_c the GL order parameter rapidly reaches its full amplitude within the grains, but phase fluctuations may still persist in granular superconductors. By further lowering the temperature the Josephson coupling energy between the grains eventually overcomes the entropy, leading to a long-range phase ordered state. This is the coherence transition, as reported in previous works[25,27] to describe the approach to the zero resistance state in polycrystalline HTSC. In this temperature region, the fluctuation conductivity is shown to diverge according to the power law

$$\Delta\sigma = A_0\left(\frac{T-T_{c_0}}{T_{c_0}}\right)^{-S}, \qquad (6)$$

where A_o is a constant and T_{c_o} is a field dependent critical temperature which denotes the establishment of the zero resistance state and S is a critical exponent related to the vortex glass physics.[27] The line through the $\chi_\sigma^{-1}(T)$ data at the left hand side of panel c) in Fig. 4, indicated by $S=3.07\pm0.05$, is a fitting to Eq. (6). Extrapolation of this line to the temperature axis yields a precise value for $Tc_0(H)$. In Fig. 7 we display the $\chi_\sigma^{-1}(T)$ data near the zero resistance state for our Zn doped single crystal in the indicated field values applied along the c axis (upper panel) or parallel to the ab
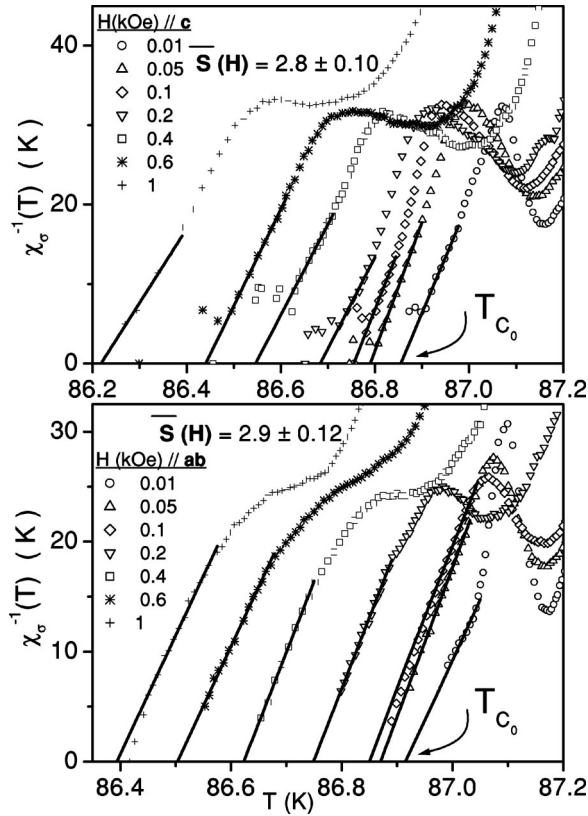
FIG. 7. The $\chi_\sigma^{-1}(T)$ data of YBCO(Zn)S2 single crystal in the approximation to zero resistance (T_{c_0}). The straight lines are fittings to the power law, Eq. (6) for the indicated fields applied parallel to the c axis (upper panel) or parallel to the ab planes (lower panel) and the $\bar{S}(H\|ab) = 2.8$ and $\bar{S}(H\|c) = 2.9$ are the respective exponents averaged over the different field values.

planes (lower panel). In the immediate vicinity of zero resistance we identify systematically the occurrence of a power law regime corresponding to the averaged exponent $\bar{S} = 2.8 \pm 0.1$, for $H\|c$ and $\bar{S} = 2.9 \pm 0.12$ for $H\|ab$. This exponent has been observed in several ceramic samples of the $HTSC$ materials in the limit of zero or very low applied field.[25–27,29,30] For most of the field intensities reported in Fig. 7, the exponents observed in polycrystalline systems

usually converge to $S \approx 4$.[25,27,31–33] We believe that the larger strength of the junctions in our single crystal as compared to that of ceramics extends the low-field regime of the coherence transition up to fields about 1 kOe, as indicated in Fig. 7.

C. Critical exponents

The contribution of the superconducting fluctuations to the electric conductivity may be described using Drude's formula combined with the GL theory.[32] Then,

$$\Delta\sigma = (2e^2/m)n_s\tau, \qquad (7)$$

where e and m are, respectively, the electron charge and mass. According to this interpretation, the divergence of $\Delta\sigma$ is governed by n_s and τ, the density of Cooper pairs and the lifetime of the evanescent superconducting fluctuations, respectively. One thus deduces that the exponent for the fluctuation conductivity close to the superconducting transition may be written as[29]

$$\lambda = \nu(2 + z - d - \mu), \qquad (8)$$

where ν is the critical exponent for the coherence length, z is the dynamical exponent, d is the dimensionality, and μ is the exponent for the order-parameter correlation function.

It is noticeable that the various fluctuation regimes observed above the pairing transition in our YBCO(Zn)S2 single crystal evolve with the applied magnetic field quite similarly as observed in a pure YBCO-123 single crystal.[33] The asymptotic region with exponent $\bar{\lambda} = 0.18 \pm 0.05$ found in zero and low applied fields is identifiable as a regime beyond 3D-XY, which has been interpreted as precursory to a weakly first order transition.[33] Estimating that the static exponents are still those of the 3D-XY universality class,[34] one deduces that the dynamical exponent has the anomalous value $z \approx 1.3$ in this temperature region. The amplitude $A_{0.18} = 2.70$ mΩ cm [Eq. (3)], obtained for the excess conductivity in this regime, is independent of the field orientation and reproduces quite closely the value found for the pure compound (see values of A^{-1} in Table I of Ref. 31). The amplitude $A_{3D-XY} = 1.18$ mΩ cm for the 3D-XY-E regime characterized by $\lambda_{cr} = 0.32$ ($\nu = 0.67, z = 1.5$, and

TABLE I. The parameters from fittings of the flux-creep (fc), de Almeida–Thouless (AT), and Gabay-Toulouse (GT) power laws to the magnetic irreversibility line.

Samples	fit	$H\|c$			$H\|ab$		
		α	H_0 (kOe)	$T_{irr}(0)$(K)	α	H_0(kOe)	$T_{irr}(0)$(K)
YBCO(Zn)-S1	fc	1.48 ± 0.06	701.84	86.3	1.52 ± 0.12	3613.91	86
	GT	0.52 ± 0.02	13.33	85.94	0.48 ± 0.13	20.87	85.64
	AT	1.49 ± 0.14	616.89	86.20	1.52 ± 0.49	410.59	86.02
YBCO(Zn)-S2	fc	1.40 ± 0.13	522.27	87.32	1.40 ± 0.16	2088.16	87.10
	GT	0.60 ± 0.09	23.13	86.88	0.54 ± 0.14	23.92	86.64
	AT	1.60 ± 0.12	934.11	87.35	1.60 ± 0.22	1269.54	87
YBCO(Mg)	fc	1.40 ± 0.10	501.02	85	1.40 ± 0.27	1979.82	84.88
	GT	0.55 ± 0.08	12.84	84.59	0.55 ± 0.23	15.34	84.14
	AT	1.55 ± 0.49	297.17	85	1.55 ± 0.49	139.71	84.88

$\mu = 0.03$)[34,35] is also independent of the field orientation and is only slightly smaller than that found in pure YBCO.[31] The fact that the critical amplitudes are unaffected by the doping indicates that the correlation length for the inhomogeneous structure, ζ_D in our sample is smaller than the temperature dependent superconducting coherence length $\xi(T) = \xi(0) \times [(T - T_c)/T_c]^{-\nu}$, in the critical fluctuation regime. From the temperature width of the critical region, which amounts to about 0.2 K, and calculating the anisotropic coherence length in this temperature range, we may estimate an upper limit for the disorder correlation length (roughly, the grain size). We obtain $\zeta_D(\|) \lesssim 90$ nm in orientations parallel to the ab planes and $\zeta_D(\perp) \lesssim 6$ nm along the c axis.

In temperatures above the range of genuine critical fluctuation, we identify Gaussian fluctuation regimes. In these temperature domains, the fluctuation conductivity is described in terms of the Aslamazov-Larkin (AL) mean field theory.[36] In our analysis we do not consider contributions from the Maki-Thompson (MT) term.[37] There is in fact a wide consensus about the absence of relevant MT contributions to the fluctuation conductivity of the HTSC near T_c.[38–44] For the AL type of divergence of the conductivity, the mean field exponents $\nu = 1/2$, $z = 2$ and $\mu = 0$ should be substituted in Eq. (8) so that $\lambda_G = (2 - d/2)$. Thus, the regime characterized by the exponent $\lambda_G^{(2D)} = 1.0$ may be attributed to two-dimensional ($d = 2$) Gaussian fluctuations. A further support for this interpretation comes from the position of the lower-temperature limit of validity of this scaling, as seen in Fig. 7. Indeed, assuming that $\xi_\perp(0) = 0.1$ nm,[31,40] we estimate that the coherence length perpendicular to the ab planes $\xi_\perp(T)$ at this temperature becomes smaller than the separation between the double CuO_2 layers in the YBCO unit cell. However, when the measured critical amplitude for this regime is compared with the theoretical expectation,[36] one obtains that the relevant layer thickness for the 2D fluctuation system amounts effectively to 3.7 nm, approximately. This is significantly larger than the value found in pure YBCO, which is 1.0 nm.[31] We attribute this difference to an effective decrease in the geometrical factor related to the fluctuation conductance of our doped sample due to its granular character. This is the "C factor" often observed to depress the amplitude of the fluctuation conductivity in some of the earliest HTSC single crystals.[45] Our assumption implies that in the Gaussian fluctuation regimes, the superconducting coherence length should be smaller than ζ_D. We remark, however, that the inhomogeneous structure that underlies the granular character of the superconducting state in our Zn-doped YBCO sample does not necessarily affect the normal transport since the absolute value of its resistivity well above T_c is not significantly modified with respect to that of the pure system.

Although large uncertainties are inherent to our method of analysis in temperatures much above T_c, where the effects of fluctuations are quite small, the systematic observation of the extended 1D-G regime with exponent $\lambda_G^{(1D)} = 1.5 \pm 0.1$ make us confident on its physical relevance. We tentatively attribute this regime to one dimensional Gaussian fluctuations. According to the Aslamazov-Larkin theory,[36] in this case the amplitude of the excess conductivity is A_{1D}

$= \pi e^2 \xi(0)/16\hbar \mathcal{A}$, where $\mathcal{A}$ is the cross sectional area of the 1D filament. From the measured amplitudes and, assuming an average value $\xi \approx 1$ nm[31] and considering the C factor equal to 3.7, as deduced from the analysis of the 2D-G regime, we obtain $\mathcal{A}^{1/2} = 2.9$ nm. This value is one order of magnitude smaller than that estimated for the in-plane coherence length $\xi_\|(T)$ at the upper temperature limit of validity for the 1D-G regime. An important point concerns the structural background underlying the one-dimensional fluctuations in YBCO. A possibility is that these fluctuations develop in 1D segments that are reminiscent of the charge-textured state typical of the stripe phases reported to occur in some cuprate superconductors.[46] Another interesting possibility is that these 1D fluctuations are related to the pseudogap phenomenon. Indeed, several experimental and theoretical investigations support the idea that the pseudogap observed in spectroscopic and thermodynamic properties of most HTSC superconductors in an extended temperature region above T_c is due to some precursory superconductivity.[47] We note that in a recent scanning tunnelling microscopy study in some $Bi_2Sr_2CaCu_2O_{8+\delta}$ crystals,[48] authors observed a pseudogap phase which appears as filamentary inclusions of similar size than the 1D fluctuations inferred from our conductivity studies.

We could not clearly discern the three-dimensional Gaussian fluctuation regime in the conductivity of our Zn-doped YBCO sample. The identification of this regime was also difficult in measurements performed in a pure YBCO crystal (see Ref. 31) since its temperature interval of validity is rather narrow.

The results in Fig. 7 deserve a final comment in this section. The observation that fluctuation magnetoconductivity diverges with exponent $S \approx 3$ in the regime describing the approach to the zero resistance state is compatible with predictions of Monte Carlo simulations by Wengel and Young[49] based on the phase-glass Hamiltonian[50]

$$H = -\sum_{i,j} J_{ij} \cos(\theta_i - \theta_j - A_{ij}), \qquad (9)$$

where J_{ij} is the Josephson coupling energy between grains i and j, θ_i and θ_j are the phases of the order parameter in grains i and j, respectively. The $A_{ij} = (2\pi/\phi_0)\int_i^j \vec{A} \cdot \vec{dl}$, where ϕ_0 is the flux quantum, are phase factors in which the line integral for the vector potential is evaluated between the centers of grains i and j. For both the gauge-glass (field-induced frustration) and chiral-glass (frustration due to randomness in the J_{ij}) versions of the model in Eq. (9), the simulations lead to the exponents $\nu = 1.3$ (as in the percolation problem) and $z = 3.1$. Supposing that μ is small in this case, these values substituted in Eq. (8) reproduce the conductivity exponent obtained from the measurements of Fig. 7. These results are indicative that the coherence transition belongs to the 3D-XY universality class with relevant disorder. In turn, the observation of the coherence transition in our Zn-doped YBCO single crystal evidences the granular character of its superconducting state.
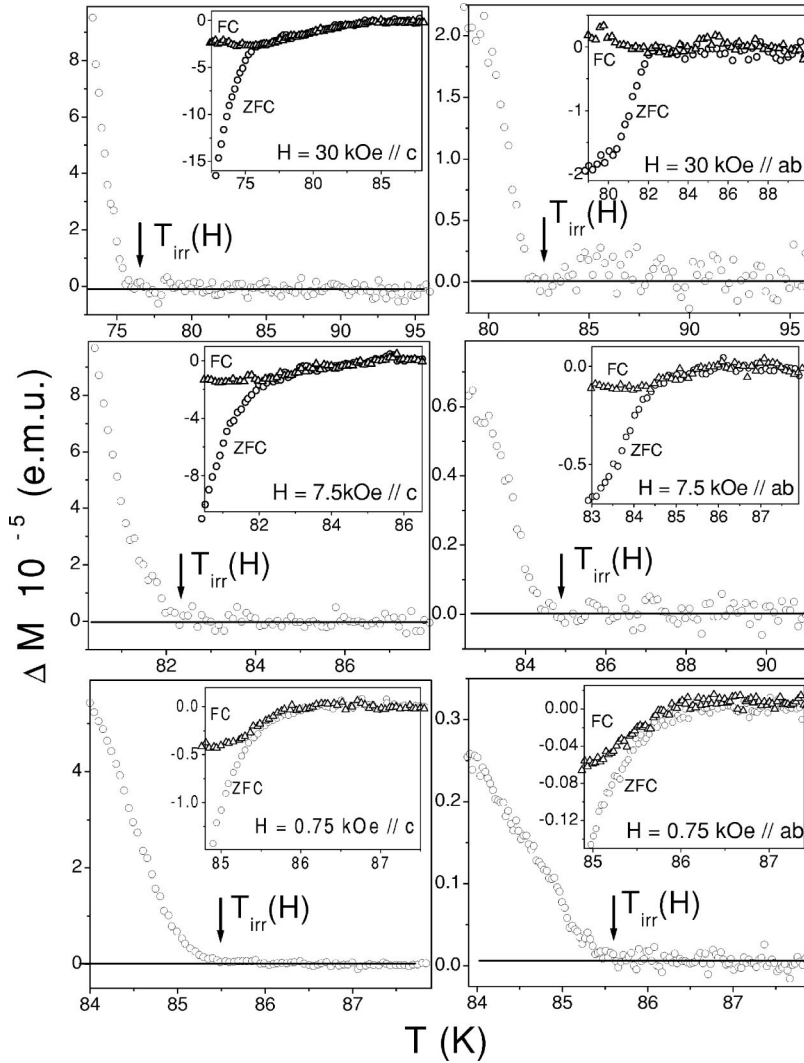
FIG. 8. The $\Delta M = M_{FC} - M_{ZFC}$ data of the YBCO(Zn)S1 single crystal exemplify our data analysis to extract the irreversibility limits. The insets show the respective M_{ZFC} and M_{FC} curves.

D. Magnetic irreversibility—Experimental results

The longitudinal magnetic moment of the pure and doped YBaCuO single crystals for fields applied parallel to the ab plane is typically one order of magnitude smaller than that obtained when the field is applied along the c axis, but still within the range of very good resolution of our SQUID magnetometer, even for low fields. We have measured the $M_{ZFC}(T)$ (zero-field-cooled) and the $M_{FC}(T)$ (field-cooled) dc magnetization curves for several fields within 0.003–50 kOe. These curves, although distinct for most of the superconducting domain, are coincident near T_c where the magnetization becomes reversible. In general these curves converge only asymptotically so that the location of the limit between the irreversible and reversible regimes is liable to considerable systematic error. This limit can nevertheless be established much more sharply in plots of the difference $\Delta M = M_{FC} - M_{ZFC}$. The irreversibility limit is the temperature point where the ΔM data abandon the zero base line defined by the data in the upper reversible temperature region. An overview of our data analysis is given in Fig. 8, where several examples of ΔM in the indicated field values and directions are plotted. The vertical arrows in this figure

indicate the irreversibility limits and the insets show the corresponding M_{ZFC} and M_{FC} data.

Plotting the irreversibility limits (T_{irr}) of a given sample for a large number of applied fields in a H-T diagram generates an irreversibility line $[T_{irr}(H)]$ that separates the H-T plane in two regions: a low temperature one, in which the flux dynamics is dissipative and thus irreversible, and a high temperature one, where the flux motion is free and the magnetization reversible. The high density and precision of our irreversibility data allowed us to put in evidence fine details of the irreversibility line. The exact form of this line is very important because it reflects much of the physics that governs the flux-dynamics in type II superconductors. Figure 9 displays the $T_{irr}(H)$ results for the YBCO(Zn)S1 ($T_c = 86.2$ K) and the YBCO(Zn)S2 ($T_c = 87.3$ K) single crystals, which are of the same batch but oxygenated at 450 °C for, respectively, seven and ten days. Analogously, Fig. 10 displays the $T_{irr}(H)$ data for the YBa$_2$Cu$_{2.97}$Mg$_{0.03}$O$_{7-\delta}$ single crystal treated in pure oxygen at 450 °C for 10 days. The insets in Figs. 9 and 10 highlight the low field details.

The magnetic irreversibility of all the samples show a considerable anisotropy for $H\|c$ and $H\|ab$ that comes from
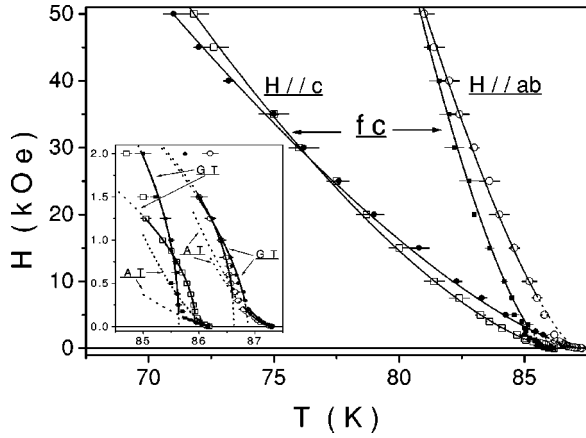
FIG. 9. The irreversibility data $T_{irr}(H)$ of our single crystals YBCO(Zn)S1 (open and closed squares) and YBCO(Zn)S2 (open and closed circles) for $H\|c$ and $H\|ab$. The continuous lines, indicated by fc are fittings to the flux-creep power law Eq. (10). The inset highlights the $T_{irr}(H)$ data in the low field range showing the characteristic marks of a frustrated superconducting grain aggregate. The continuous lines through the data in the insets are fittings to the de Almeida–Thouless (AT) and the Gabay-Toulouse (GT) power laws. Remark the effect of the different oxygen contents.

the intrinsic planar structure of these materials. The continuous lines labeled fc through the data in the high field region are fittings with the power law

$$H_{irr}(T)=H_0^{fc}(1-t^{fc})^\alpha \qquad \left(\alpha=\frac{3}{2}\right), \qquad (10)$$

where $H_{irr}(T)$ is the irreversibility field as a function of the temperature, $t^{fc}=T_{irr}^{fc}(H)/T_{irr}^{fc}(0)$ is the reduced temperature, and H_0^{fc} as well as $T_{irr}^{fc}(0)$ are fitting parameters (see Table I). This power law arises within the conventional flux-creep (fc) theories.[51,52] However, the $T_{irr}(H)$ data of our single crystals doped with Zn or Mg fit to Eq. (10) only in fields above 2 kOe.

The continuous lines through the data in the lowest field part of the insets in Figs. 9 and 10, labeled AT, are fittings to
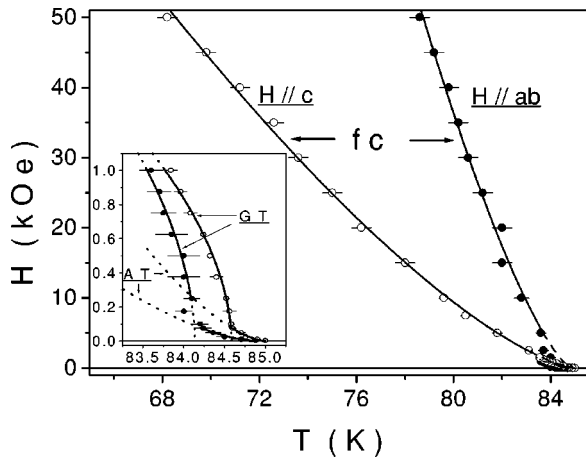

FIG. 10. The same as in Fig. 9 but for the YBa$_2$Cu$_{2.97}$Mg$_{0.03}$O$_{7-\delta}$ single crystal.

the de Almeida–Thouless (AT) like power law,[53] which was originally deduced from mean-field calculations for frustrated Ising like spin glasses. The AT line has the same form as Eq. (10) but with different fitting parameters. We label these parameters as H_0^{AT} and $T_{irr}^{AT}(0)$ in Table I in order to clearly distinguish them from the corresponding ones in the fc formula. For field values about 0.1 kOe the $T_{irr}(H)$ data suddenly change slope and bend in the opposite sense for increasing fields. The continuous lines through these data up to about 1.5 kOe are fittings with the Gabay-Toulouse (GT-) like power law[54]

$$H=H_0^{GT}(1-t^{GT})^\alpha \qquad \left(\alpha=\frac{1}{2}\right). \qquad (11)$$

This power law is known from mean-field calculations for frustrated XY or Heisenberg spin-glass systems. Here $t^{GT}=T_{irr}^{GT}(H)/T_{irr}^{GT}(0)$ is the reduced temperature and H_0^{GT} and $T_{irr}^{GT}(0)$ are fitting parameters listed in Table I.

As observed in YBa$_{2-x}$Sr$_x$Cu$_3$O$_{7-\delta}$ (Ref. 55) here also the planar anisotropy of the magnetic irreversibility in the low field region (AT and GT range) is reversed with respect to that in high fields (fc range). However, besides the planar anisotropy we observe that the slope of the irreversibility line also depends on the oxygen content as well as on the chemical property of the dopand atoms. While in the high field range this slope is steeper in the oxygen poor YBCO(Zn)S1 and the YBa$_2$Cu$_{2.97}$Mg$_{0.03}$O$_{7-\delta}$ single crystals, it does the opposite in the low field range, see also Refs. 26 and 56.

E. Magnetic irreversibility—Discussion

In homogeneous superconductors the magnetic-flux dynamics is expected to follow the prospects of the conventional flux-creep theories.[51,52] A very pure and untwinned YBa$_2$Cu$_3$O$_{7-\delta}$ single crystal behaves approximately as such a homogeneous superconductor. In conformity with this its magnetic irreversibility line is well fitted by the power law given by Eq. (10) in the whole field range.[55] Quite differently, however, the magnetic irreversibility data of our doped YBa$_2$Cu$_{2.97}$M$_{0.03}$O$_{7-\delta}$ (M=Zn or Mg) single crystals can be fitted to Eq. (10) only in fields above 2 kOe, regardless its orientation with respect to the crystal axes. Below this field value the $T_{irr}(H)$ data fall systematically off this power law and conform to the AT and GT power law regimes, characteristic of frustrated systems. The occurrence of these power law regimes together with the observation of a coherence transition in the resistive transition indicates that our doped crystals behave as disordered and frustrated granular superconductors. We remind that the superconducting-glass[57] and the vortex-glass[58] models predict the existence of such frustrated systems.

We explain the more conventional behavior of the magnetic irreversibility above 2 kOe by assuming that in this field range the flux-dynamics is dominated by the intragrain Abrikosov vortices, and that within the grains this flux sees an almost homogeneous superconducting medium. In low fields, however, the flux dynamics is dominated by the intergranular Josephson flux that is related to the very inhomoge-

neous superconducting medium formed by the multiconnected array of weakly coupled superconducting grains.

In the superconducting glass model,[57] the aggregate of superconducting grains is usually described by the effective Hamiltonian of Eq. (9) to which a charge energy term is added:[56,59,60]

$$H = -2e^2 \sum_{ij} n_i n_j C_{ij}^{-1} - \sum_{\langle i,j \rangle} J_{i,j} \cos(\theta_i - \theta_j - A_{ij}),$$
(12)

where C_{ij} in the Coulomb term is an element of the capacitance matrix for the granular array and n_i, n_j are the number of electron pairs on grains i and j, respectively.

The Coulomb charge energy term plays the role of a random anisotropy that suppresses local degrees of freedom for vortex fluctuations within the range of the AT-like regime. We believe that the crossover from the AT-like to the GT-like regimes occurs when the magnetic energy brought by the applied field is enough to collapse these local anisotropies, giving place to vortex fluctuations of higher dimensionality. This is an analogy to the well-known phenomenology of spin glasses[61] where a strong enough applied field collapses the random local anisotropy fields causing an Ising-XY or an Ising-Heisenberg crossover that originates the observed de Almeida-Thouless to Gabay-Toulouse power law crossover in the magnetic irreversibility of these systems.[62] Our observations suggest that on lowering the temperature the superconducting grain aggregate freezes into a highly degenerate ground state having many energy minima of nearly the same value. This is characteristic of disorder and frustration that underlies the behavior of the Josephson flux dynamics and the magnetic irreversibilities of granular superconductors such as our Zn or Mg-doped YBCO single crystals.

In the recent STM study prior referred,[48] the differential conductance (gap) was mapped out over the surface of $Bi_2Sr_2CaCu_2O_{8-\delta}$ single crystals at low temperatures. The resulting gap maps show a well-defined granular structure on the whole surface of the crystals. In an underdoped sample, low-gap islands of about 3 nm in size are imbedded in a background of high-gap material. In another sample, the high-gap material meanders as filamentary inclusions about the low-gap domains. These maps provide a direct verification of the intrinsic electronic inhomogeneity of these HTSC and are believed to correlate to a random stoichiometry of oxygen within the samples. Probably, the distribution of the oxygen doping is related to that of impurities and lattice defects in general. The aggregate of low-gap islands have been suggested to represent a system of coupled superconducting grains. The high-gap domains are interpreted as a pseudogap phase. This is in qualitative agreement with the picture that emerges from our magnetoresistivity and magnetic irreversibility studies at low applied fields in the present work as well as in previous ones.[26,55] However, we should also notice that these same works put into evidence that the magnetic flux properties in fields higher than a few thousand of Oe goes over into the conventional description of the Abrikosov-flux lattice in a homogeneous superconducting medium. This is totally inconceivable if the size of the superconducting grains are within the nanometer scale because there can hardly be place for more than one fluxon within each grain. Several hypotheses to conciliate these findings are possible. For instance, as suggested by our fluctuation conductivity results, a possibility exists that the superconducting grains in our doped YBCO single crystals are comparatively larger than those in the Bi-based superconductors. It is also possible that the electronic granularity evidenced by the STM studies in Ref. 48 evolves with increasing field and temperature into large homogeneous superconducting regions. A detailed irreversibility study of Bi-based single crystals is thus clearly wanted.

Another important aspect arises when comparing the irreversibility data of the samples with different oxygen contents or substitutions of Cu by different chemical elements. While in high fields the slopes of $T_{irr}(H)$ lines for $H\|c$ as well as for $H\|ab$ of the oxygen poor YBCO(Zn)S1 sample are steeper than those of the well oxygenated YBCO(Zn)S2 sample, in low fields the slopes of the AT and GT curves do the very opposite, see Fig. 9 and Table I. The magnetic irreversibility limit is a measure of the pinning strength. While an increase of the number of oxygen holes improves pinning of the Abrikosov-flux within the grains, it drastically deteriorates the grain junctions that pin the Josephson flux. On the other hand, while changing the Zn atoms for Mg has a subtle effect on the intragrain flux dynamics, it is very drastic on the intergranular flux dynamics. It in fact has the same profile as an oxygen deficiency. Apparently the Mg impurities impede full oxygenation of the samples. All these effects are clearly reflected by the fitting parameters in Table I, but see also Figs. 9 and 10.

In conclusion our magnetoresistivity studies put in evidence the relevance of the superconducting granularity in the configuration of the superconducting properties of Zn (Mg) doped YBCO single crystals. On the other hand, the $T_{irr}(H)$ data, besides verifying the intragrain Abrikosov-flux-dynamics in the major high field region, they also evidence the existence of a dominant intergranular Josephson-flux dynamics in a low-field high-temperature region, which bears the frustrated grain coupling physics. They also verify the effects of oxygen underdoping and the chemical properties of the impurities at the Cu sites on the pinning strength within the grains and grain junctions.

*Email address: schaf@if.ufrgs.br

[1] R.S. Howland, T.H. Geballe, S.S. Laderman, A. Fischer-Colbrie, M. Scott, J.M. Tarascon, and P. Barboux, Phys. Rev. B **39**, 9017 (1989).

[2] C.Y. Yang, A.R. Moodenbaugh, Y.L. Wang, Y. Xu, S.M. Heald, D.O. Welch, M. Suenaga, D.A. Fischer, and J.E. Penner-Hahn, Phys. Rev. B **42**, 2231 (1990).

[3] K. Semba, A. Matsuda, and T. Ishii, Phys. Rev. B **49**, 10 043 (1994).

[4] R. Liang, T. Nakamura, H. Kawaji, M. Itoh, and T. Nakamura, Physica C **170**, 307 (1990).

[5] Y. Saito, T. Noji, A. Endo, N. Higuchi, K. Fujimoto, T. Oikawa, A. Hattori, and K. Fukuse, Physica B **148**, 336 (1987).

[6] L. Raffo, R. Caciuffo, D. Rinaldi, and F. Licci, Supercond. Sci. Technol. **8**, 409 (1995).

[7] W.M. Tiernan, R.B. Hallok, J.C.W. Chien, and B.M. Gong, Phys. Rev. B **44**, 4661 (1991).

[8] T. Komatsu, H. Meguro, R. Sato, O. Tanaka, K. Matusita, and T. Yamashita, Jpn. J. Appl. Phys. **27**, L2063 (1988).

[9] J. Figueras, T. Puig, A.E. Carrilllo, and X. Abrados, Supercond. Sci. Technol. **13**, 1067 (2000).

[10] Y. Tatsumi, T. Kebukawa, Y. Misawa, and K. Fujiwara, Jpn. J. Appl. Phys. **31**, L392 (1992).

[11] P. Mendels, J. Bordoff, G. Collin, H. Alloul, M. Gabay, J.F. Marucco, N. Blanchard, and B. Grenier, Europhys. Lett. **46**, 678 (1999).

[12] R.P. Gupta and M. Gupta, Phys. Rev. B **59**, 3381 (1999).

[13] B. Nachumi, A. Keren, K. Kojima, M. Larkin, G.M. Luke, J. Merrin, O. Tchernyshv, Y.J. Uemura, N. Ichikawa, M. Goto, and S. Uchida, Phys. Rev. Lett. **77**, 5421 (1996).

[14] C. Bernhard, J.L. Tallon, C. Bucci, R. de Renzi, G. Guidi, G.V.M. Williams, and Ch. Niedermayer, Phys. Rev. Lett. **77**, 2304 (1996).

[15] K. Tomimoto, I. Terasaki, A.I. Rykov, T. Mimura, and S. Tajima, Phys. Rev. B **60**, 114 (1999).

[16] T.R. Chien, Z.Z. Wang, and N.P. Ong, Phys. Rev. Lett. **67**, 2088 (1991).

[17] D.L. Sisson, S.G. Doettinger, A. Kapitulnik, R. Liang, D.A. Bonn, and W.N. Hardy, Phys. Rev. B **61**, 3604 (2000).

[18] J. W Loram, K.A. Mirza, and P.F. Freeman, Physica C **171**, 243 (1990).

[19] H. Alloul, P. Mendels, H. Casalta, J.F. Marucco, and J. Arabski, Phys. Rev. Lett. **67**, 3140 (1991).

[20] S. Adachi, C. Kasai, S. Tajioma, K. Tanabe, S. Fujihara, and T. Kimura, Physica C **351**, 323 (2001).

[21] K. Ishida, Y. Kitaoka, N. Ogata, T. Kamino, K. Asayama, J.R. Cooper, and N. Athanassopoulou, J. Phys. Soc. Jpn. **62**, 2803 (1993).

[22] J. Axns, W. Holm, Yu. Eltsev, and O. Rapp, Phys. Rev. B **53**, R3003 (1996).

[23] A.J. Zaleski and J. Klamut, Phys. Rev. B **59**, 14 023 (1999).

[24] C. Panagopoulos, J.R. Cooper, N. Athanassopoulou, and J. Chrosch, Phys. Rev. B **54**, R12 721 (1996).

[25] A.R. Jurelo, I.A. Castillo, J. Roa-Rojas, L.M. Ferreira, L. Ghivelder, P. Pureur, and P. Rodrigues, Jr., Physica C **311**, 133 (1999).

[26] V.N. Vieira, J.P. da Silva, and J. Schaf, Phys. Rev. B **64**, 094516 (2001).

[27] J.R. Rojas, R.M. da Costa, P. Pureur, and P. Prieto, Phys. Rev. B **61**, 12 457 (2000).

[28] C.J. Lobb, Phys. Rev. B **36**, 3930 (1987).

[29] J. Rosenblatt, in *Percolation, Localization and Superconductivity*, NATO ASI Series, edited by A. M. Goldman and S. A. Wolf (Plenum, New York, 1984) p. 431; J. Rosenblatt, P. Peyral, A. Raboutou, and C. Lebeau, Physica B **152**, 95 (1988).

[30] A.R. Jurelo, J.V. Kunzler, J. Schaf, and P. Pureur, Phys. Rev. B **56**, 14 815 (1997).

[31] R.M. Costa, P. Pureur, M. Gusmo, S. Senoussi, and K. Behnia, Phys. Rev. B **64**, 214513 (2001); Solid State Commun. **113**, 23 (1999).

[32] F.W. Fabris, J. Roa-Rojas, and P. Pureur, Physica C **354**, 304 (2001).

[33] P. Pureur, R.M. Costa, P. Rodrigues, Jr., J. Schaf, and J.V. Kunzler, Phys. Rev. B **47**, 11 420 (1993).

[34] J.C. Le Guillou and J. Zinn-Justin, Phys. Rev. B **21**, 3976 (1980).

[35] C. Hohenberg and B.I. Halperin, Rev. Mod. Phys. **49**, 435 (1977).

[36] L.G. Aslamazov and A.I. Larkin, Sov. Phys. Solid State **10**, 875 (1968).

[37] K. Maki and R.S. Thompson, Phys. Rev. B **39**, 2767 (1989).

[38] P.P. Freitas, C.C. Tsuei, and T.S. Plasket, Phys. Rev. B **36**, 833 (1987).

[39] M. Ausloos, P. Clippe, and Ch. Laurent, Phys. Rev. B **41**, 9506 (1990).

[40] T.A. Friedmann, J.P. Rice, J. Giapintzakis, and D.M. Gisnberg, Phys. Rev. B **39**, 4258 (1989).

[41] P. Pureur, R.M. Costa, P. Rodrigues, Jr., J. Schaf, and J.V. Kunzler, Phys. Rev. B **50**, 9456 (1994).

[42] J. Vieira and F. Vidal, Phys. Rev. B **42**, 8748 (1990).

[43] A. Pomar, M.V. Ramallo, J. Mosqueira, C. Torrn, and F. Vidal, Phys. Rev. B **54**, 7470 (1996).

[44] W. E. Lawrence and S. Doniach, (unpublished).

[45] S.J. Hagen, Z.Z. Wang, and N.P. Ong, Phys. Rev. B **38**, 7137 (1988).

[46] J.M. Tranquada, J.D. Axe, N. Ichikawa, Y. Nakamura, S. Uchida, and B. Nachumi, Phys. Rev. B **54**, 7489 (1996).

[47] T. Timusk and B. Statt, Rep. Prog. Phys. **62**, 61 (1999).

[48] K.M. Lang, V. Madhavan, J.E. Hoffman, E.W. Hudson, H. Eisaki, S. Uchida, and J.C. Davis, Nature (London) **415**, 412 (2002).

[49] C. Wengel and A.P. Young, Phys. Rev. B **56**, 5918 (1997).

[50] M.P.A. Fischer, T.A. Tokuyasu, and A.P. Young, Phys. Rev. Lett. **66**, 2931 (1991).

[51] P.W. Anderson and Y.B. Kim, Rev. Mod. Phys. **36**, 39 (1964).

[52] Y. Yeshurun and A.P. Malozemoff, Phys. Rev. Lett. **60**, 2202 (1988).

[53] J.R.L. de Almeida and D.J. Thouless, J. Phys. A **11**, 983 (1978).

[54] M. Gabay and G. Toulouse, Phys. Rev. Lett. **47**, 201 (1981).

[55] V.N. Vieira and J. Schaf, Phys. Rev. B **65**, 144531 (2002).

[56] P. Rodrigues, Jr., J. Schaf, and P. Pureur, Phys. Rev. B **49**, 15 292 (1994).

[57] W.Y. Shih, C. Ebner, and D. Stroud, Phys. Rev. B **30**, 114 (1984); **31**, 165 (1985).

[58] M.P.A. Fisher, Phys. Rev. Lett. **62**, 1415 (1989).

[59] F.V. Kusmartsev, Phys. Rev. Lett. **69**, 2268 (1992).

[60] B.I. Spivak and S.A. Kivelson, Phys. Rev. B **43**, 3740 (1991).

[61] G.G. Kenning, D. Chu, and R. Ohrbach, Phys. Rev. Lett. **66**, 2923 (1991).

[62] G. Kotliar and H. Sompolinsky, Phys. Rev. Lett. **53**, 1751 (1984).